UC San Diego
International Symposium on Stratified Flows

Title
Thermohaline layering in dynamically and diffusively stable shear flows

Permalink
https://escholarship.org/uc/item/94x6h9jw

Journal
International Symposium on Stratified Flows, 1(1)

Author
Radko, Timour

Publication Date
2016-08-31

eScholarship.org Powered by the California Digital Library
University of California

Thermohaline layering in dynamically and diffusively stable shear flows[1]

Timour Radko
Department of Oceanography
Naval Postgraduate School
Monterey, CA 93943
tradko@nps.edu

Abstract

In this study we examine two-component shear flows that are stable with respect to Kelvin-Helmholtz and to double-diffusive instabilities individually. Our focus is on the diffusively stratified ocean regions, where relatively warm and salty water-masses are located below cool and fresh. It is shown that such systems may be destabilized by the interplay between shear and thermohaline effects, caused by unequal molecular diffusivities of density components. Linear stability analysis suggests that parallel two-component flows can be unstable for Richardson numbers exceeding the critical value for non-dissipative systems ($Ri = ¼$) by up to four orders of magnitude. Direct numerical simulations indicate that these instabilities transform the initially linear density stratification into a series of well-defined horizontal layers.

1. Introduction

This study contributes to the discussion of the origin of thermohaline staircases in high-latitude regions of the World Ocean. The term thermohaline staircase describes a series of mixed layers separated by thin high-gradient interfaces, commonly observed in vertical profiles of temperature and salinity. Staircases in the Arctic and Southern Oceans are typically diffusive, which means that warm and salty water is located below cold and fresh, and they often exhibit remarkable spatial and temporal coherence (e.g., Timmermans et al., 2008).

Despite the profound importance of staircases for high-latitude ocean dynamics (Turner, 2010; Flanagan et al., 2013) the physical cause of diffusive layering has not been fully explained (Kelley et al., 2003; Radko, 2013). It is generally accepted that staircases are ultimately produced and maintained by double-diffusive processes. A major challenge in the development of a complete theory of high-latitude staircases is explaining the initiation of layering and diffusive convection from smooth original distribution of temperature and salinity. The parameter range for diffusive instability in the ocean is extremely narrow (e.g., Walin, 1964; Veronis, 1965):

$$1 < R_\rho < \frac{\mathrm{Pr}+1}{\mathrm{Pr}+\tau}, \qquad (1)$$

where R_ρ is the diffusive density ratio – the ratio of vertical gradients of temperature and salinity, normalized by the expansion/contraction coefficients; $\tau = \frac{k_S}{k_T}$ is the diffusivity ratio; $\mathrm{Pr} = \frac{\nu}{k_T}$ is the Prandtl number. Here k_T and k_S are the molecular diffusivities of temperature and salinity; ν is the molecular viscosity. For oceanic parameters ($\tau \sim 0.01$, $\mathrm{Pr} \sim 10$) condition (1) reduces to $1 < R_\rho < 1.1$, and this interval lies outside of the density ratio range typical for oceanic diffusive staircases ($1.5 < R_\rho < 10$). Typical internal wave energy and associated vertical shears in the Arctic at the staircase depth range (150-300m) are also weak (e.g., Cole et al., 2014). As a result, the representative values of Richardson number (*Ri*) – the measure of flow susceptibility to

[1] This contribution represents an abbreviated version of the manuscript which is currently under review by JFM.

dynamic instability – are high ($Ri \sim 10$), substantially exceeding the threshold value of $Ri = \frac{1}{4}$ required for dynamic instability. Hence, the background stratification is generally stable with respect to both primary diffusive and dynamic instabilities.

To rationalize the propensity for layering in stably stratified waters, we argue that even when a two-component flow is stable with respect to dynamic and diffusive instabilities individually, it may become unstable due to the interplay between shear and thermohaline effects. This conclusion is supported by a Floquet-based stability analysis for a sinusoidal velocity profile in a fluid linearly stratified in the diffusive sense. Direct numerical simulations (DNS) indicate that the combined thermohaline-shear instabilities can indeed trigger the transition of uniformly stratified systems to well-defined staircases.

2. Formulation

The temperature and salinity fields (T_{tot}, S_{tot}) are separated into uniform vertical background gradients (T_{bg}, S_{bg}) and a departure (T, S) from it. Consider the basic state representing unidirectional shear flow with a sinusoidal velocity profile:

$$\overline{u}(z) = U_0 \sin\left(\frac{2\pi z}{H}\right), \quad \overline{\mathrm{v}} = \overline{w} = \overline{T} = \overline{S} = 0. \tag{2}$$

It is assumed that the shear (2) is maintained against viscous dissipation by the externally imposed pressure gradient force and the governing Boussinesq equations are non-dimensionalized using H as the unit of length and U_0 as the unit of velocity. The non-dimensionalization is implemented as follows:

$$\begin{aligned} &(u, \mathrm{v}, w) \to U_0 (u, \mathrm{v}, w), \quad p \to \rho_0 U_0^2 p, \\ &(x, y, z) \to H(x, y, z), \quad t \to \frac{H}{U_0} t, \\ &\alpha T \to \alpha \left|\frac{\partial T_{bg}}{\partial z}\right| HT, \quad \beta S \to \alpha \left|\frac{\partial T_{bg}}{\partial z}\right| HS, \end{aligned} \tag{3}$$

which transforms the governing equations to

$$\begin{cases} \dfrac{\partial T}{\partial t} + \vec{\mathrm{v}}_{tot} \cdot \nabla T - w_{tot} = \dfrac{1}{Pe} \nabla^2 T \\ \dfrac{\partial S}{\partial t} + \vec{\mathrm{v}}_{tot} \cdot \nabla T - R_\rho w_{tot} = \dfrac{\tau}{Pe} \nabla^2 S \\ \dfrac{\partial \vec{\mathrm{v}}_{tot}}{\partial t} + \vec{\mathrm{v}}_{tot} \cdot \nabla \vec{\mathrm{v}}_{tot} = -\nabla p_{tot} + \dfrac{4\pi^2 Ri}{R_\rho - 1} (T - S)\vec{k} + \dfrac{\mathrm{Pr}}{Pe} \nabla^2 \vec{\mathrm{v}}_{tot} \\ \nabla \cdot \vec{\mathrm{v}}_{tot} = 0, \end{cases} \tag{4}$$

where $R_\rho = \dfrac{(\beta S_{bg})_z}{(\alpha T_{bg})_z}$ is the background density ratio, $Ri = \dfrac{N_b^2 H^2}{4\pi^2 U_0^2} = \alpha \left|\dfrac{\partial T_{bg}}{\partial z}\right| \dfrac{gH^2}{4\pi^2 U_0^2} \left(R_\rho - 1\right)$ is the minimal Richardson number and N_b is the buoyancy frequency, $Pe = \dfrac{U_0 H}{k_T}$ is the Peclet number, $\tau = \dfrac{k_S}{k_T}$ is the diffusivity ratio, and $\mathrm{Pr} = \dfrac{\nu}{k_T}$ is the Prandtl number.

3. Direct numerical simulations

Preliminary insights into the thermohaline-shear destabilization were first generated from numerical solutions. The governing equations (4) were integrated in time using the dealiased pseudospectral method (e.g., Stern et al. 2001; Stellmach et al. 2011) with periodic boundary conditions applied for the perturbation fields in each spatial direction.

Figure 1 presents a typical 2D simulation. The chosen parameters $\left(Ri, R_\rho, Pe\right) = \left(10, 2, 100\right)$ define a system that is individually stable with respect to dynamic and to diffusive instabilities. This calculation was initiated by the basic state (2) perturbed by small-amplitude random initial (T,S) distribution. The computational domain $\left(L_x, L_z\right) = (64, 64)$ was resolved by the numerical mesh with 6144×6144 grid points. The evolution of this system is illustrated by a sequence of temperature perturbation snapshots (Figs. 1a-d). The instability which forms first is relatively small-scale – its dominant vertical scale conforms to the periodicity of the basic shear (Fig. 1a). In time, however, layers merge sequentially and their number reduces from $N = 64$ at $t = 1009$ (Fig. 1a) to $N = 6$ at $t = 3968$ (Fig. 1d).

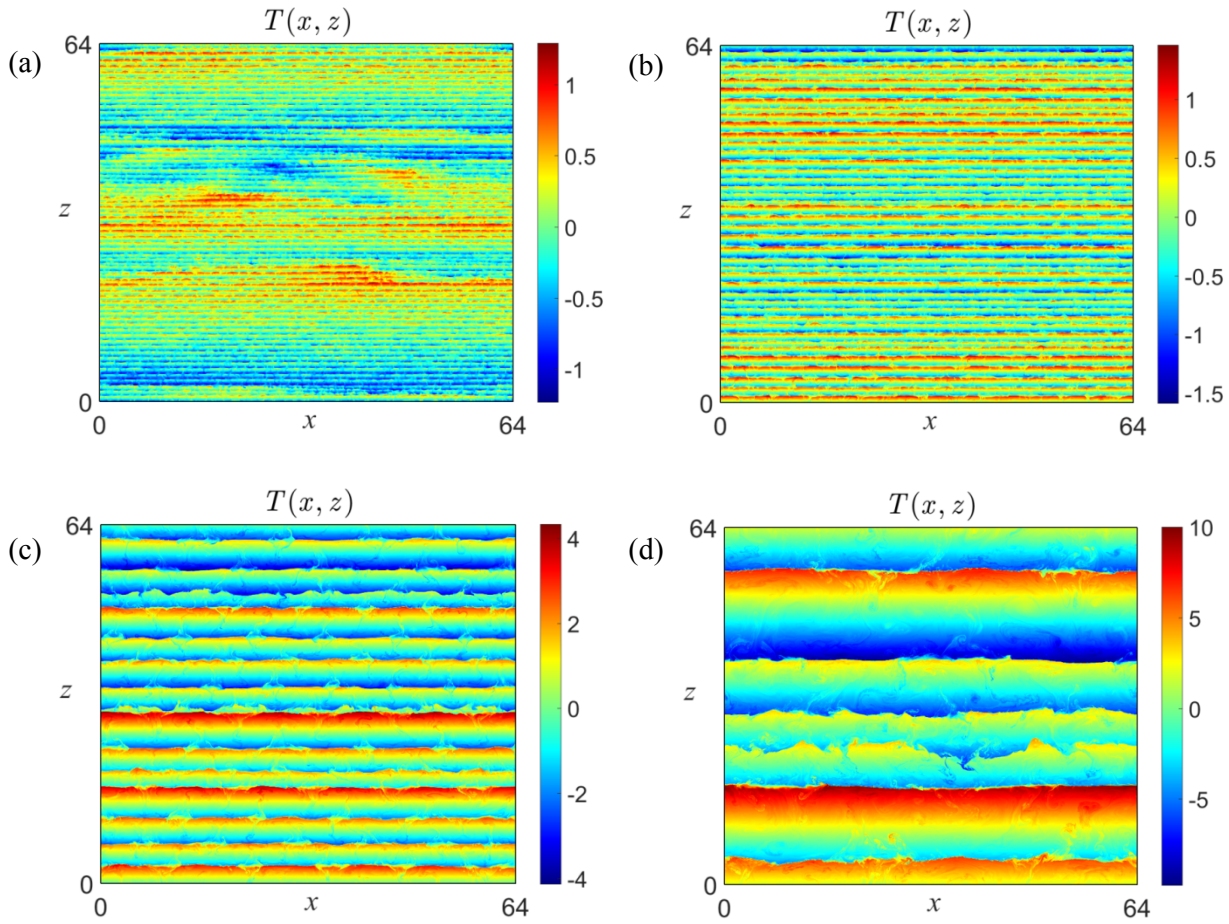

Figure 1. Two-dimensional DNS for $\left(R_\rho, Ri, Pe, \tau\right) = \left(2, 10, 10^2, 0.01\right)$. The instantaneous temperature perturbations are shown for $t = 1009,\ 2005,\ 3500,\ 3969$ in (a)-(d) respectively.

4. Linear stability analysis

To systematically examine stability properties of the doubly-stratified shear flow, the governing equations were linearized with respect to the basic state and the solution was sought in the following form, suggested by the Floquet theory:

$$\begin{pmatrix} T \\ S \\ u \\ \mathrm{v} \\ w \\ p \end{pmatrix} = \exp(ikx + ily + im_f z + \lambda t) \sum_{n=-N}^{N} \begin{pmatrix} T_n \\ S_n \\ u_n \\ \mathrm{v}_n \\ w_n \\ p_n \end{pmatrix} \exp(inz), \tag{5}$$

where λ is the growth rate; k and l are the horizontal wavenumbers; and m_f is the Floquet coefficient, which controls the fundamental wavelength in z. When (5) is substituted into the linearized governing equations and the individual Fourier components are collected, the stability problem reduces to the matrix form:

$$\lambda\vec{\xi} = \boldsymbol{A}\vec{\xi}, \tag{6}$$

where

$$\vec{\xi} = (T_{-N}, S_{-N}, u_{-N}, v_{-N}, w_{-N}, p_{-N}, \ \ldots, T_N, S_N, u_N, v_N, w_N, p_N). \tag{7}$$

and $\boldsymbol{A}$ is the $(12N+2)\times(12N+2)$ matrix, whose elements are functions of $k, l, m_f, Pe, R_\rho, Ri, N$.

For each set of governing parameters, the eigenvalue with the maximum real part determines the growth rate of the most rapidly amplifying mode. Extensive experimentation with the model indicated that, in all cases considered, the most rapid growth occurs when the Floquet factor is zero. This means that the fastest growing mode of instability has the same periodicity as that of the shear and $m_f = 0$ will be used in subsequent calculations. Likewise, testing the model's performance for different resolutions indicated that N=100 is sufficient for an accurate representation of the thermohaline-shear instabilities in the considered parameter range and it will be employed hereafter. Figure 2 presents the plot of maximal growth rates, in logarithmic coordinates, as a function of (Pe, Ri) for various density ratios (R_ρ). The reduction in R_ρ has a destabilizing effect on the system. The parameter space occupied by unstable modes tends to be very wide at low density ratios ($R_\rho = 1.5$ and $R_\rho = 2$ in Figs. 2a,b) and contracts with the increasing R_ρ ($R_\rho = 10$ and $R_\rho = 50$ in Figs. 2c,d). Likewise, the thermohaline-shear instability is sensitive to the diffusivity ratio (not shown).

5. Energetics

One of the key questions in the analysis of the thermohaline-shear instability is the ultimate source of energy required to amplify the unstable perturbations. The answer to this question is by no means obvious. The source of energy of Kelvin-Hemholtz instability is the kinetic energy of the basic shear, whereas double-diffusion is driven by the release of potential energy stored in the unstably stratified density component. To identify the energy source for the mixed thermohaline-shear instabilities, the (non-dimensional) perturbation energy equation was obtained for the linearized system of governing equations:

$$\frac{\partial E}{\partial t} = P_{dd} + P_{sh} + P_{visc}, \tag{8}$$

where

$$
\begin{aligned}
E &= \int\left(\frac{u^2+\mathrm{v}^2+w^2}{2}+\frac{4\pi^2 Ri}{(R_\rho-1)^2}\frac{(S-T)^2}{2}\right)dV,\\
P_{dd} &= \frac{4\pi^2 Ri}{Pe(R_\rho-1)^2}\int(S-T)\nabla^2(\tau S-T)dV,\\
P_{sh} &= -\int\frac{\partial\overline{u}}{\partial z}uwdV,\\
P_{visc} &= -\frac{\mathrm{Pr}}{Pe}\int\left(\left|\nabla u\right|^2+\left|\nabla \mathrm{v}\right|^2+\left|\nabla w\right|^2\right)dV.
\end{aligned}
\tag{9}
$$

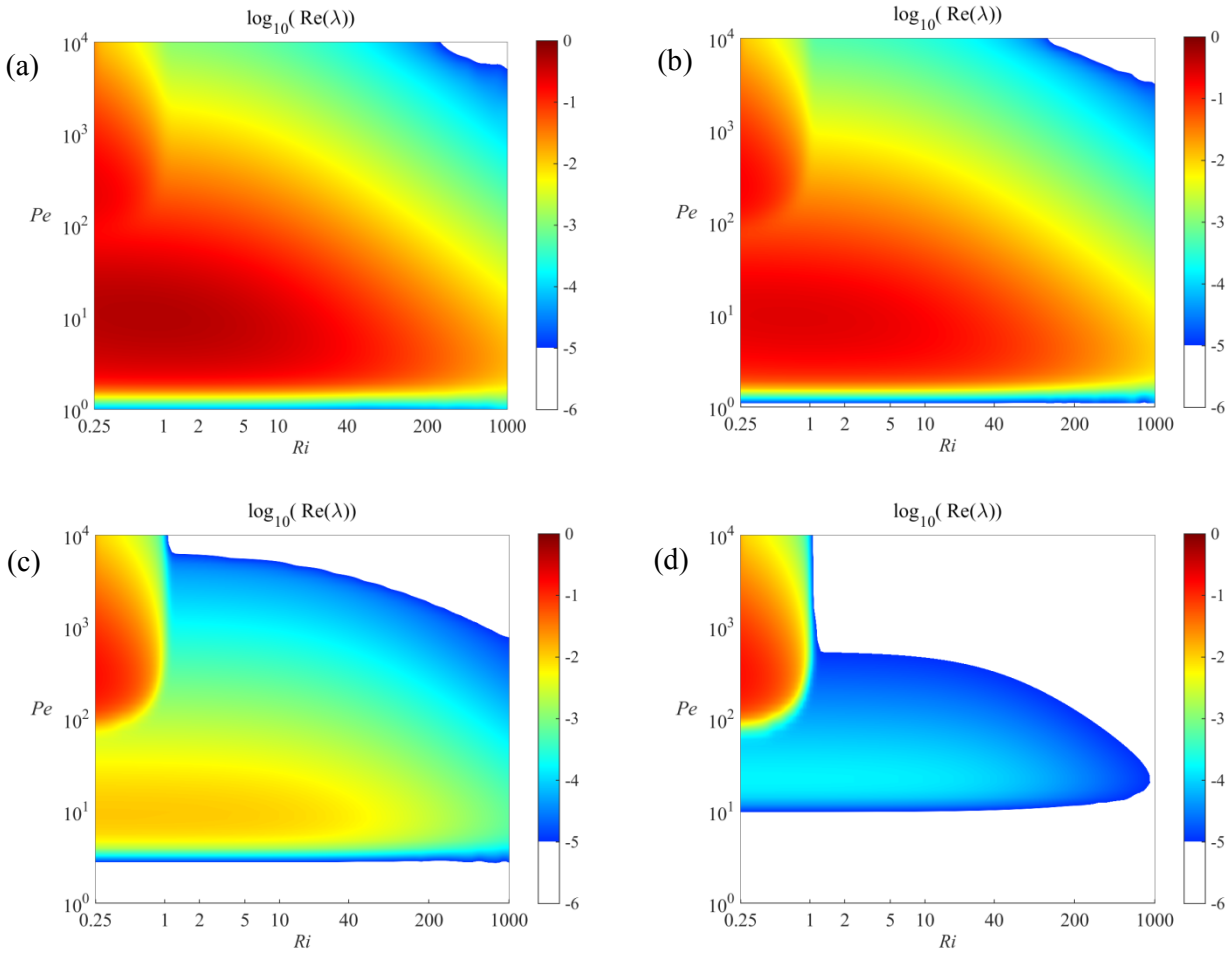

Figure 2. The decimal logarithm of the maximal growth rate $\log_{10}(\mathrm{Re}(\lambda))$ is plotted as a function of (Ri, Pe) for $R_\rho = 1.5,\ 2,\ 10,\ 50$ in (a)-(d) respectively for $\tau = 0.01$. Only the growth rates exceeding 10^{-5} are shown. Note the reduction in the intensity of thermohaline-shear instability with the increasing density ratio.

The P_{dd} term in (8) represents the production of perturbation energy by diffusion of heat and salt, P_{sh} is interpreted as the production of energy by shear, and P_{visc} is the viscous dissipation.

Finally, the individual terms in (8) were evaluated for the fastest growing normal modes identified using the Floquet-based analysis in Sec. 4. Of particular interest was the relative contribution of double-diffusive, shear-driven, and viscous energy production/dissipation mechanisms. The answer turned out to be regime-dependent. Figure 3 shows the variation in the energy balance for a series of calculations in which *Pe* was systematically increased, whereas all other governing parameters were kept constant $(R_\rho, Ri, \tau) = (2, 1, 0.01)$. The relative contribution of various processes is quantified by plotting

$$\left(P_{dd\ rel}, P_{sh\ rel}, P_{visc\ rel}\right) = \frac{\left(P_{dd}, P_{sh}, P_{visc}\right)}{P_{dd} + P_{sh} + P_{visc}} \tag{10}$$

as a function of *Pe*. These diagnostics highlight the stark differences between the low-*Pe* and high-*Pe* regimes, which were evident in DNS and in the linear stability analyses (Sec. 4). For high Peclet numbers ($Pe > 500$) the dominant energy balance is between the energy production by the basic shear and its viscous dissipation. Nevertheless, double-diffusion still accounts for a surprisingly large fraction of energy production ($P_{dd\ rel} = 0.55 - 0.65$). The reason for such high double-diffusive contribution is that much of perturbation kinetic energy produced by shear is immediately dissipated by viscosity.

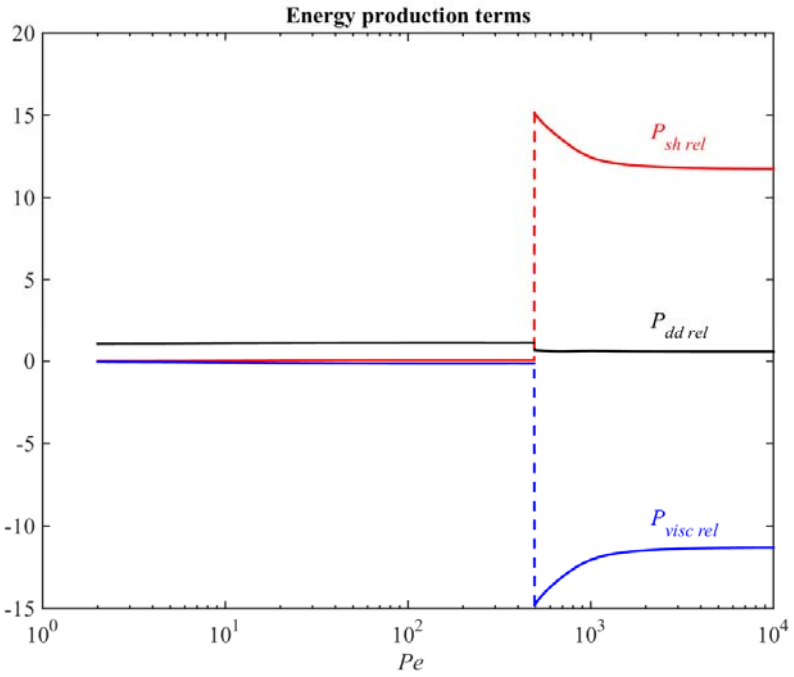

Figure 3. The energy production/dissipation balances for various values of *Pe*. Note the existence of two dynamically dissimilar regimes: (i) the high-Pe regime ($Pe > 500$) in which the dominant balance is between the production of the perturbation energy by shear and its viscous dissipation, and (ii) the low-Pe regime ($Pe < 500$) in which the energy released by the unstable basic temperature gradient is transferred directly into the perturbation field.

Dynamics of low-*Pe* systems are dissimilar. The perturbation energy is produced almost entirely by double-diffusion ($P_{dd\ rel} = 1.05 - 1.1$). The shear-driven contribution is small ($P_{sh\ rel} = 0.01 - 0.05$) and so is the viscous dissipation ($-P_{visc\ rel} = 0.05 - 0.15$). This result, however, should be interpreted with caution. Even though shear-induced effects are not strongly reflected in the energetics, it would be erroneous to conclude that they are largely irrelevant for the dynamics of thermohaline systems at low *Pe*. On the contrary, the release of potential energy by double-diffusion is only possible due to the catalytic role of shear. In the absence of shear, the smooth thermohaline stratification in the oceanographically relevant parameter regime would be linearly stable.

6. Discussion

Some of the most fascinating problems in instability theory arise when two independently stable processes lead to the destabilization of systems concurrently affected by both. A well-known example of this counterintuitive behavior is the unstable system consisting of a vertically bounded uniform shear and bottom-heavy stratification, each of which is stable individually (Richardson, 1920). Other cases that fall into the same category include the joint instability of rotating magnetic fields that are separately stable (Stern, 1963) and the instability of a stable thermal stratification in the presence of a nominally stabilizing magnetic field (Hughes and Weiss, 1995). Our study offers yet another example of such unexpected destabilization – the dynamically and diffusively stable two-component shear flows. Linear stability analysis based on the Floquet theory demonstrates that shear flows can be unstable for surprisingly high values of density ratio ($R_\rho \sim 10$) and Richardson number ($Ri \sim 10^3$). These values greatly exceed the individual thresholds for both dynamic and diffusive instabilities $\left(R_{\rho\,cr}, Ri_{cr}\right) = \left(1.1, 0.25\right)$. Such a wide parameter range for thermohaline-shear instability includes typical parameters of the ocean regions characterized by thermohaline layering.

Thermohaline-shear instability exhibits many interesting and, in several ways, counterintuitive features. Depending on the parameter regime, the most rapidly amplifying unstable modes can be localized in low-shear or high-shear regions and yet the presence of shear is absolutely essential. The thermohaline-shear instability rapidly intensifies with decreasing *Ri*, R_ρ and τ . As with Kelvin-Helmholtz instability, the most rapidly amplifying perturbations are aligned in the direction normal to the flow. The transition to fully three-dimensional patterns occurs only at the nonlinear evolutionary stages, characterized by the appearance of secondary instabilities. Multiple lines of evidence – stemming from DNS, Floquet stability analysis, and arguments based on energetics – indicate the existence of two dynamically distinct regimes, realized for low and high Peclet numbers. The low-*Pe* regime is perhaps more interesting since the dissimilarities with the one-component systems here are most profound. In both cases, most of the energy required for perturbation growth is supplied by the unstably stratified density component (*T*). In this regard, the thermohaline-shear instability is similar to double-diffusion, with shear flow playing a catalytic role in the amplification of perturbations. In the high-*Pe* case, however, a large amount of energy is supplied by the basic shear, but this gain is compensated by the equivalent energy loss due to viscous dissipation.

Finally, it should be emphasized that the effects discussed in this study should not be considered as merely an example of fluid-dynamical curiosity. Fully nonlinear simulations reveal that the thermohaline-shear instability can reorganize smooth *T*-*S* fields into a series of mixed layers separated by thin high-gradient interfaces. These structures are suggestive of diffusive staircases, commonly observed in high-latitude regions of the World Ocean (Arctic and Southern Oceans), which raises an intriguing question whether the origin of staircases can be attributed to the thermohaline-shear instability. In this regard, an important caveat of our analysis is the steady state model of the background shear. The steady state assumption made it possible to perform

formal linear stability analysis in a straightforward manner and efficiently explore the parameter space. However, in the ocean, vertical finescale shear is largely associated with the internal wave field and therefore it is neither steady nor unidirectional. It would be of interest to determine whether the thermohaline-shear instability persists in the stochastic wave-driven shears (e.g., Radko et al., 2015) and whether it produces layering as effectively as its steady-state counterpart.

References

Cole, S. T., M. L. Timmermans, J. M. Toole, R. A. Krishfield and F. T. Thwaites, 2014: Ekman veering, internal waves, and turbulence observed under Arctic sea ice. *J. Phys. Oceanogr.*, **44**, 1306-1328.

Flanagan, J., A. Lefler and T. Radko, 2013: Heat transport through diffusive interfaces. *Geophys. Res. Lett.,* **40**, 2466-2470.

Hughes, D. W., and N. O. Weiss, 1995: Double-diffusive convection with two stabilizing gradients: strange consequences of magnetic buoyancy. *J. Fluid Mech*., **301**, 383-406.

Kelley, D. E., H. J. S. Fernando, A. E. Gargett, J. Tanny., and E. Ozsoy, 2003: The diffusive regime of double-diffusive convection. *Progress Oceanogr*., **56**, 461-481.

Radko, T., 2013: *Double-Diffusive Convection*. New York: Cambridge University Press. 344pp.

Radko, T., J. Ball, J. Colosi and J. Flanagan, 2015: Double-diffusive convection in a stochastic shear. *J. Phys. Oceanogr*., **45**, 3155-3167.

Richardson, L. F., 1920: The supply of energy from and to atmospheric eddies. *Proc. Roy. Soc.* A, **97**, 354−373.

Stellmach, S., A. Traxler, P. Garaud, N. Brummell and T. Radko, 2011: Dynamics of fingering convection II: The formation of thermohaline staircases. *J. Fluid Mech*., **677**, 554-571.

Stern, M. E., 1963: Joint instability of hydromagnetic fields which are separately stable. *Phys. Fluids*, **6**, 636–642.

Stern, M. E., T. Radko, and J. Simeonov, 2001: 3D salt fingers in an unbounded thermocline with application to the Central Ocean. *J. Mar. Res.*, **59**, 355–390.

Timmermans, M.-L., J. Toole, R. Krishfield, and P. Winsor, 2008: Ice-Tethered Profiler observations of the double-diffusive staircase in the Canada Basin thermohaline. *J. Geophys. Res*., **113**, C00A02.

Turner, J. S., 2010: The melting of ice in the Arctic Ocean: The influence of double-diffusive transport of heat from below. *J. Phys. Oceanogr*., **40**, 249-256.

Veronis, G., 1965: On finite amplitude instability in thermohaline convection. *J. Marine Res*., **23**, 1-17.

Walin, G., 1964: Note on stability of water stratified by both salt and heat. *Tellus*, **18**, 389–393.